Single-photon transport through a waveguide coupling to a quadratic optomechanical system

Lei Qiao
School of Physics, Peking University, Beijing 100871, China
and Collaborative Innovation Center of Quantum Matter, Beijing 100871, China
(Received 26 December 2016; published 31 July 2017)

We study the coherent transport of a single photon, which propagates in a one-dimensional waveguide and is scattered by a quadratic optomechanical system. Our approach, which is based on the Lippmann-Schwinger equation, gives an analytical solution to describe the single-photon transmission and reflection properties. We analyze the transport spectra and find they are not only related to the optomechanical system's energy-level structure, but also dependent on the optomechanical system's inherent parameters. For the existence of atomic degrees of freedom, we get a Rabi-splitting-like or an electromagnetically induced transparency (EIT)-like spectrum, depending on the atom-cavity coupling strength. Here, we focus on the single-photon strong-coupling regime so that single-quantum effects could be seen.

DOI: 10.1103/PhysRevA.96.013860

I. INTRODUCTION

Single photons are considered as one of the most suitable carriers of quantum information due to the relative low decoherence over a long distance in the waveguide. It is important to control and manipulate the single-photon transport in quantum communication and quantum computation. In recent years, the single-photon transport properties controlled by interaction with the local coupled two- or multilevel system in a one-dimensional (1D) waveguide have been extensively investigated both theoretically [1–6] and experimentally [7–10]. It is found that a photon with frequency resonant with a coupled two-level atom can be reflected with high probability. Indeed, 94% extinction of the transmitted photon has been observed experimentally in the circuit QED system [11]. Compared to a two-level system, a multilevel system provides more controllable parameters and more options for photons to transmit or reflect. Nowadays, a controllable photon transport system can be realized in different ways, such as a 1D superconducting transmission line coupled to a single artificial atom [11], surface plasmons confined on a conducting nanowire coupled to a single two-level emitter [12], or a photonic nanowire with an embedded quantum dot [13].

Recently, cavity optomechanics, which is the study of coherent coupling between electromagnetic and mechanical degrees of freedom, has been a burgeoning field [14–17]. There have been a number of theoretical proposals and experimental realizations probing the optomechanical coupling property [18,19]. Most of the studies focus on the linear optomechanical coupling (LOC), which means that the interaction is proportional to the displacement of the mechanical oscillator. These LOC interactions have been used for many aspects, such as entanglement between microwave fields and the mechanical oscillator [20], optomechanically induced transparency [21], and optomechanical normal-mode splitting [22]. The nonlinear effects in multimode optomechanical systems with LOC are also explored [23,24]. However, the interaction with quadratic optomechanical coupling has been demonstrated [25–27]. In these systems, a micromechanical membrane or ultracold atoms are introduced. Though the currently attainable quadratic coupling strength between the optomechanical membrane and the cavity field is weak, much attention has been paid to this area. And, recently, some methods have been proposed to increase the interaction or to seek other possible realization of quadratic optomechanics [28–30] which provide a possibility to observe the quantum characteristics of the quadratic strong-coupling system. Also, various phenomena based on the quadratic optomechanical coupling, such as photon blockade [31], macroscopic tunneling in optomechanical double-well potential [32], and two-phonon cooling of the mechanical oscillator [33] have been proposed.

Typically, in most quantum optomechanical devices, the cavity is direct or side coupled to a waveguide [19]. Thus, in the single-photon regime, optomechanical systems, rather than traditional quantum emitters [2,3], may enable us to control single-photon propagation in the waveguide. Moreover, the single-photon transport spectra can be used to probe the optomechanical system's inherent parameters and characterize its energy-level structure.

Motivated by the advances in the quadratic optomechanical system, in this paper, we investigate theoretically the single-photon transport in a 1D waveguide coupled to a local quadratic optomechanical system which is coupled by a two-level atom, as shown in Fig. 1. Such quadratic optomechanical systems have been studied in recent papers [34,35]. Here, we employ a full quantum mechanical approach, which is based on the Lippmann-Schwinger equation, to study the transmission and reflection properties of a photon propagating in the waveguide. An analytical solution to the transport spectra is derived. We analyze the connection between the spectral features and the system's energy-level structure, and present how the spectra characterize the single-photon strong-coupling regime. The conditions for the sideband peaks to be visible are clarified. For the existence of atomic degrees of freedom, we get a Rabi-splitting-like or an electromagnetically induced transparency (EIT)-like spectrum, depending on the atom-cavity coupling strength. In our treatment, it is assumed that the system works in a single-photon strong-coupling regime, where multiple phonons are involved in the scattering. So, single-quantum effects could be seen in this regime.

The paper is organized as follows. In Sec. II, we introduce the model of single-photon transport and give the calculation method and the solutions to the model. In Sec. III, we study the single-photon transport properties when the optomechanical

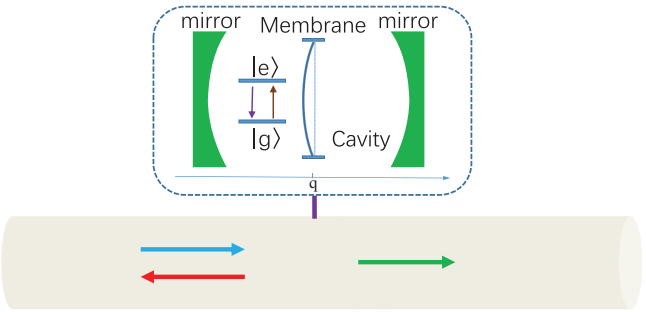

FIG. 1. The schematic diagram of the transport model. A 1D waveguide is side coupled by the hybrid atom-optomechanical system and the single photon propagates along the arrow direction in the waveguide.

system contains no atom and a two-level atom. Finally, we summarize the single-photon transport and give the conclusions in Sec. IV.

II. HAMILTONIAN AND SOLUTIONS

A. The model and Hamiltonian

As shown in Fig. 1, the system we consider contains a 1D waveguide and a quadratic optomechanical system which is coupled by a two-level atom. Usually, the hybrid atom-optomechanical system can be either side coupled or direct coupled to a waveguide. In this paper, we consider the side-coupled case, as shown in Fig. 1, for the transport coefficient of the direct-coupled case, which can be straightforwardly obtained by mapping the reflection amplitude of the side-coupled case into the transmission amplitude of the direct-coupled case [3]. The optomechanical system is formed by a single-mode cavity and a thin dielectric membrane with mass M. The membrane and the cavity field are coupled to each other via radiation pressure. When the membrane is located at a node of the intracavity standing wave, the cavity field can quadratically couple to the mechanical motion of the membrane. In this case, the cavity field frequency $\omega_a(q)$ can be approximated to the second order of the membrane's displacement q: $\omega_a(q) = \omega_a + \gamma q^2$ with $\gamma = \frac{1}{2}\frac{\partial^2\omega_a(q)}{\partial q^2}|_{q=0}$. Let $a^\dagger(a)$ be the creation (annihilation) operator of the cavity field; then the Hamiltonian of the optomechanical system can be written as (with $\hbar = 1$)

$$H_{\rm opc} = \omega_a(q)\left(a^\dagger a + \frac{1}{2}\right) + \frac{p^2}{2M} + \frac{1}{2}M\Omega_M^2 q^2, \qquad (1)$$

where p is the membrane's momentum and Ω_M is the vibration frequency of the membrane. By introducing the mechanical creation (annihilation) operator $b^\dagger(b)$ and writing $q = \sqrt{\frac{1}{2M\omega_M}}(b^\dagger + b)$, $p = i\sqrt{\frac{M\omega_M}{2}}(b^\dagger - b)$ with $\omega_M = \sqrt{\Omega_M^2 + \gamma/M}$, the Hamiltonian becomes [25]

$$H_{\rm opc} = \omega_a a^\dagger a + \omega_M b^\dagger b + g_0 a^\dagger a(b^\dagger + b)^2, \qquad (2)$$

where $g_0 = \frac{\gamma}{2M\omega_M}$ is the quadratic optomechanical coupling strength between the cavity field and the membrane. Let us denote the Fock state $|i\rangle_a$ as the state of the cavity field and the Fock state $|n\rangle_b$ as the state of the membrane; then the eigenequation of the Hamiltonian $H_{\rm opc}$ can be derived as [36,37]

$$H_{\rm opc}|i\rangle_a|\tilde{m}(i)\rangle_b = (\omega_a i + m\omega_{Mi} + \delta_i)|i\rangle_a|\tilde{m}(i)\rangle_b. \qquad (3)$$

Here, $\omega_{Mi} = \omega_M\sqrt{1 + \frac{4g_0 i}{\omega_M}}$ is the i-photon coupled resonant frequency of the membrane and $\delta_i = \frac{1}{2}(\omega_{Mi} - \omega_M)$ is the frequency shift. $|\tilde{m}(i)\rangle_b$ is the one-photon squeezed phonon number state of the membrane and is defined by

$$|\tilde{m}(i)\rangle_b = S_b(\eta_i)|m\rangle_b, \qquad (4)$$

where $S_b(\eta_i) = \exp[\frac{\eta_i}{2}(b^2 - b^{+2})]$ is a squeezing operator with the squeezing factor $\eta_i = \frac{1}{4}\ln(1 + \frac{4g_0 i}{\omega_M})$. One can see that the membrane has a different energy-level structure when the cavity contains different number of photons.

The two-level atom is characterized by a ground state $|g\rangle$ and an excited state $|e\rangle$. Here, we set the ground energy to be zero as reference and let Ω be the energy of the excited state. The Hamiltonian of the whole system can be written as

$$H = H_0 + V$$

and

$$H_0 = \int dk\omega_k c_k^\dagger c_k + \Omega|e\rangle\langle e| + \omega_a a^\dagger a + \omega_M b^\dagger b + g_0 a^\dagger a(b^\dagger + b)^2, \qquad (5)$$

$$V = \lambda(a\sigma^+ + \sigma^- a^+) + \int dk J(c_k a^\dagger + a c_k^\dagger), \qquad (6)$$

where c_k ($c_k^\dagger$) is the annihilation (creation) operator for the kth-mode electromagnetic field with frequency ω_k in the waveguide and $\omega_k = v_g|k|$. Here, v_g is the group velocity of light. $\sigma^+ = |e\rangle\langle g|$ ($\sigma^- = |g\rangle\langle e|$) is the atomic raising (lowering) operator. λ is the coupling strength between the cavity field and the atom. The second term in Eq. (6) represents the coupling between the waveguide and the atom-optomechanical system, and J is the coupling strength. The cavity-waveguide decay rate can be defined as $\Gamma = \frac{2\pi J^2}{v_g}$ [4]. In our treatment, it is assumed that the majority of the decayed light from the cavity is guided into the waveguide modes [38,39], i.e., strong coupling exists between the cavity and the waveguide. Thus the decay rate κ of the cavity into channels except the waveguide is negligible. In addition, the dissipation rate γ_M of the membrane is assumed to be much smaller than Γ, λ, g_0, so we neglect the membrane's dissipation process.

B. The Lippmann-Schwinger equation and scattering amplitudes

Let us assume that the membrane is initially in the number state $|n_0\rangle_b$ when a single photon with energy ω_k is incident from the left of the 1D waveguide, and take the input state as $c_k^\dagger|\emptyset\rangle|n_0\rangle_b$. Here, $|\emptyset\rangle = |0\rangle_k|0\rangle_a|g\rangle$ is the vacuum state which indicates that there is zero photon in both the waveguide and the cavity and that the atom is in the ground state $|g\rangle$. Then the scattering state $|\psi_{kn_0}^{(+)}\rangle$ is given by the Lippmann-Schwinger equation [40,41] as

$$|\psi_{kn_0}^{(+)}\rangle = c_k^\dagger|\emptyset\rangle|n_0\rangle_b + \frac{1}{\omega_{k,n_0} - H_0 + i0^+}V|\psi_{kn_0}^{(+)}\rangle, \qquad (7)$$

where $\omega_{k,n_0} = \omega_k + n_0\omega_M$ represents the energy of the incident state of the system.

Since the excitation number $N = \int dk c_k^\dagger c_k + a^\dagger a + |e\rangle\langle e|$ is conserved in this system, the eigenstate with $N = 1$ can be written as

$$|\psi_{kn_0}^{(+)}\rangle = \sum_n \int dp u_p(n) c_p^\dagger |\emptyset\rangle|n\rangle_b + \sum_n \alpha_k(n) a^\dagger |\emptyset\rangle|\tilde{n}(1)\rangle_b + \sum_n \beta_k(n)\sigma^+|\emptyset\rangle|n\rangle_b. \quad (8)$$

For simplicity, the one-photon squeezed phonon number state $|\tilde{n}(1)\rangle_b$ is denoted as $|\tilde{n}\rangle_b$ in the following. These squeezed number states in Eq. (8) satisfy the orthogonality $\langle\tilde{m}|_b|\tilde{n}\rangle_b = \delta_{m,n}$, and the completeness $\sum_{n=0}^{\infty}|\tilde{n}\rangle_b\langle\tilde{n}|_b = I$. Besides, the overlap between the harmonic-oscillator number state $|m\rangle_b$ and the squeezed number state $|\tilde{n}\rangle_b$ is determined by the relation [31,42]

$$\langle m|_b|\tilde{n}\rangle_b = \frac{\sqrt{m!n!}}{(\cosh\eta_1)^{n+1/2}} \sum_{l'=0}^{\mathrm{Floor}[\frac{m}{2}]} \sum_{l=0}^{\mathrm{Floor}[\frac{n}{2}]} \frac{(-1)^{l'}}{l!l'!} \times \frac{\left(\frac{1}{2}\tanh\eta_1\right)^{l+l'}}{(n-2l)!}(\cosh\eta_1)^{2l}\delta_{m-2l',n-2l}, \quad (9)$$

where the function Floor$[x]$ means the greatest integer less than or equal to x. It is noted that the Kronecker δ function $\delta_{m-2l',n-2l}$ in Eq. (9) requires that m and n should have the same parity, i.e., being odd or even, otherwise $\langle m|_b|\tilde{n}\rangle_b = 0$.

By substituting Eq. (7) into Eq. (8), one can obtain

$$u_p(m) = \delta(p-k)\delta_{m,n_0} + J\sum_{n'}\langle m|_b|\tilde{n}'\rangle_b\alpha_k(n') \times \frac{1}{\omega_{k,n_0} - \omega_p - m\omega_M + i0^+}, \quad (10)$$

$$\alpha_k(m) = \frac{J\langle\tilde{m}|_b|n_0\rangle_b}{\omega_{k,n_0} - (\omega_a + m\omega_{M1} + \delta_1) - \frac{\lambda^2}{\omega_{k,n_0} - \Omega - m\omega_M} + i\Gamma}, \quad (11)$$

with $\Gamma = \frac{2\pi J^2}{v_g}$.

For calculating the single-photon transport coefficient, we rewrite the scattering state in real space as

$$|\psi_{kn_0}^{(+)}\rangle = \sum_n \int_{-\infty}^{+\infty} dx u(x,n) c^\dagger(x)|\emptyset\rangle|n\rangle_b + \sum_n \alpha_k(n) a^\dagger|\emptyset\rangle|\tilde{n}(1)\rangle_b + \sum_n \beta_k(n)\sigma^+|\emptyset\rangle|n\rangle_b, \quad (12)$$

where

$$c^\dagger(x) = \int_{-\infty}^{+\infty} dp \frac{e^{-ixp}}{\sqrt{2\pi}} c_p^\dagger, \quad (13)$$

$$u(x,n) = \int dp \frac{e^{ixp}}{\sqrt{2\pi}} u_p(n). \quad (14)$$

By combining Eqs. (10) and (14), one can get the photon wave function $u(x,n)$. In fact, to study the transport problem, we only need to know the wave function in the limit $|x| \to \infty$ [40],

$$u(x,n) = \begin{cases} \frac{e^{ikx}}{\sqrt{2\pi}}\delta_{n,n_0} + \frac{e^{-ikx}}{\sqrt{2\pi}} r_n(k), & x \to -\infty \\ \frac{e^{ikx}}{\sqrt{2\pi}} t_n(k), & x \to +\infty, \end{cases} \quad (15)$$

where $k_n > 0$ and satisfy the relation $v_g k_n = \omega_{k,n_0} - n\omega_M$. r_n (t_n) is the reflection (transmission) amplitude,

$$r_n(k) = -\frac{2\pi i J}{v_g}\sum_{n'}\langle n|_b|\tilde{n}'\rangle_b\alpha_k(n'), \quad (16)$$

$$t_n(k) = \delta_{nn_0} - \frac{2\pi i J}{v_g}\sum_{n'}\langle n|_b|\tilde{n}'\rangle_b\alpha_k(n'). \quad (17)$$

The single-photon scattering process can be formulated as follows. The hybrid atom-optomechanical system initially prepared in the state $|\emptyset\rangle|n_0\rangle_b$ absorbs the incident photon with frequency ω_k, and emits an outgoing photon with frequency ω_{k_n} when the state of the atom-optomechanical system is changed to $|\emptyset\rangle|n\rangle_b$. The frequency of the outgoing photon meets the relation $v_g k_n = \omega_{k,n_0} - n\omega_M$, which is consistent with the law of energy conservation. Note that the photon is scattered into a mixed state because of the contribution of the phonon state with $n \neq n_0$. Each pure-state component corresponds to a phonon Fock state. For the nth pure-state component, the transmittance is $|t_n|^2$ and the reflectance is $|r_n|^2$. Thus, the total single-photon transmission and reflection coefficients can be written as

$$T(k) = \sum_n |t_n(k)|^2, \quad R(k) = \sum_n |r_n(k)|^2. \quad (18)$$

Using Eqs. (11) and (16)–(18), we numerically calculate the total single-photon transmission and reflection coefficients, from which the probability current conservation relation, i.e., $T(k) + R(k) = 1$, is confirmed.

More generally, when the membrane is initially prepared in a pure state $\sum_{n_0=0}^{\infty} C_{n_0}|n_0\rangle_b$ or a mixed state $\sum_{n_0=0}^{\infty} P_{n_0}|n_0\rangle_b\langle n_0|_b$, the total transmission and reflection coefficients are given, respectively, by

$$T(k) = \sum_{n=0}^{\infty}\left|\sum_{n_0=0}^{\infty} C_{n_0} t_{n_0,n}(k)\right|^2,$$

$$R(k) = \sum_{n=0}^{\infty}\left|\sum_{n_0=0}^{\infty} C_{n_0} r_{n_0,n}(k)\right|^2, \quad (19a)$$

$$T(k) = \sum_{n=0}^{\infty}\sum_{n_0=0}^{\infty} P_{n_0}\left|t_{n_0,n}(k)\right|^2,$$

$$R(k) = \sum_{n=0}^{\infty}\sum_{n_0=0}^{\infty} P_{n_0}\left|r_{n_0,n}(k)\right|^2. \quad (19b)$$

For a thermal equilibrium state, $P_{n_0} = \bar{n}_b^{n_0}/(\bar{n}_b+1)^{n_0+1}$, where $\bar{n}_b$ is the average phonon occupation number.

III. SINGLE-PHOTON SCATTERING SPECTRA

A. Single-photon transport coefficient with no atom in the optomechanical cavity

First, we investigate the case of no atom in the optomechanical cavity. The transport results of this case can be acquired by setting $\lambda = 0$ and $\Omega = 0$ in the equations above. It is known that the single-photon squeezing operator $S_b(\eta_1) = \exp[\frac{\eta_1}{2}(b^2 - b^{+2})]$, which is produced due to the quadratic optomechanical coupling between the cavity field and the membrane, causes the transitions between different Fock states of the membrane. If we take the limit $\eta_1 \to 0$, which means that the coupling strength g_0 between the cavity field and the membrane is absent, the squeezing operator can be expanded to the lowest order, i.e., $S_b(\eta_1) \simeq 1$. When the membrane is initially prepared in an arbitrary Fock state $|n_0\rangle_b$, the reflection coefficient in this limit case reduces to the Lorentzian line shape that is the same as the case of the local coupled quantum bit [1],

$$R(k) = \frac{\Gamma^2}{(\omega_k - \omega_a)^2 + \Gamma^2}, \tag{20}$$

and the transmission coefficient reduces to

$$T(k) = \frac{(\omega_k - \omega_a)^2}{(\omega_k - \omega_a)^2 + \Gamma^2}. \tag{21}$$

It is clear that the probability current conservation relation $R(k) + T(k) = 1$ holds. Note that Eqs. (20) and (21) have nothing to do with the initial state of the membrane because of the absence of the coupling between the cavity field and membrane. Therefore, there is only one resonance which is located at $\omega_k = \omega_a$. As the coupling strength g_0 increases, the scattering state of the incident photon can be more affected by the state of the membrane. If we keep up the squeezing operator to the first two orders, $\exp[\frac{\eta_1}{2}(b^2 - b^{+2})] \simeq 1 + \frac{\eta_1}{2}(b^2 - b^{+2})$, the optomechanical system may absorb the incident photon and, meanwhile, the membrane gains two phonons, loses two phonons (if $n_0 > 2$), or remains in the original state. Notice that the energy levels of the membrane have been shifted and renormalized due to the radiation pressure when the cavity contains a photon [see Eq. (3)]. As a result, the outgoing photon is in a mixed state consisting of three components, one of which has the resonance energy $\omega_k = \omega_a + n_0\omega_{M1} + \delta_1 - n_0\omega_M$; the other two have the resonance energy $\omega_k = \omega_a + (n_0 - 2)\omega_{M1} + \delta_1 - n_0\omega_M$ and $\omega_k = \omega_a + (n_0 + 2)\omega_{M1} + \delta_1 - n_0\omega_M$. As g_0 becomes larger, more orders of the squeezing operator come into effect. So the higher-order phonon processes take place.

In Fig. 2, we plot the single-photon transmission and reflection coefficients as functions of the incident photon frequency ω_k while the membrane is initially prepared in the ground state $|0\rangle_b$. It is observed in Fig. 2(a) that the reflection peak, whose width is $\Gamma/\omega_M = 0.2$, occurs at the resonant point $\omega_k/\omega_M = \omega_a/\omega_M = 2$ and no phonon sideband peaks can been seen. As the coupling strength g_0 increases to be comparable to the mechanical frequency ω_M, as shown in Figs. 2(b) and 2(c), we see that the location of the zeroth-order (main) reflection peak (or transmission dip) has shifted from ω_a/ω_M to $(\omega_a + \delta_1)/\omega_M$. This feature may be used as the controllable quantum switch for the coherent transport of a single photon [2] if the coupling strength could be changed in quantum devices [43]. The location of the first-order peak is at $(\omega_a + 2\omega_{M1} + \delta_1)/\omega_M$. The spacing between the zeroth-order and first-order peaks becomes bigger when g_0 increases, which is different from the linear case in which the spacing is fixed at ω_M [44]. By comparing Figs. 2(c) and 2(d), we see that even though the system works in the single-photon strong-coupling regime, there are no sideband peaks in the spectrum when the value of Γ/ω_M changes from 0.2 to 1.5. We found that in the case of $\Gamma > \omega_M$, the phonon-sideband evidence is negligible. Such a condition can be understood by examining the height and width of these peaks in the spectrum. To resolve a peak, the peak height should be much higher than the tail of its neighboring one. When $\Gamma > \omega_M$, the zeroth-order peak becomes too wide and covers the first-order peak. In this paper, we consider $\Gamma < \omega_M$ as the resolved-sideband condition. Thus, both the strong-coupling condition and the resolved-sideband condition are required for observing sideband peaks in the reflection spectra.

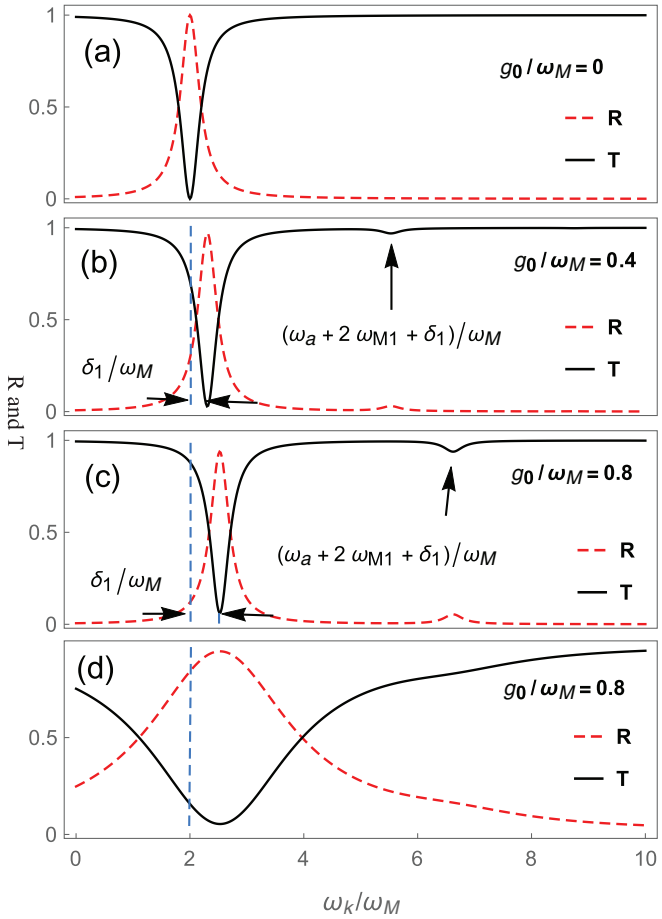

FIG. 2. Single-photon transmission spectra and reflection spectra with $\lambda = 0$ for various values of g_0 and Γ. The membrane's initial state is $|0\rangle_b$. The parameter $\omega_a/\omega_M = 2$. (a)–(c) are plotted with $\Gamma/\omega_M = 0.2$, while (d) is plotted with $\Gamma/\omega_M = 1.5$.

B. Single-photon transport coefficient with a two-level atom in the optomechanical cavity

We next consider the case in which the optomechanical cavity is coupled by a two-level atom. To investigate the

single-photon transmission and reflection properties, we first calculate the eigenvalues and eigenstates of the hybrid atom-optomechanical system. The system Hamiltonian is given by

$$\tilde{H}_{AO} = \tilde{H}_0 + \tilde{H}_I, \tag{22}$$

where

$$\tilde{H}_0 = \Omega|e\rangle\langle e| + \omega_a a^+ a + \omega_M b^+ b + g_0 a^+ a(b^+ + b)^2, \tag{23}$$

$$\tilde{H}_I = \lambda(a|e\rangle\langle g| + |g\rangle\langle e|a^+). \tag{24}$$

One can get the eigenstates and eigenvalues as

$$|m,+\rangle = \sin\frac{\theta}{2}|g\rangle|1_a\tilde{m}_b\rangle + \cos\frac{\theta}{2}|e\rangle|0_a m_b\rangle, \tag{25}$$

which corresponds to the eigenenergy

$$E_{m,+} = \frac{E_{m,1}+E_{m,2}}{2} + \frac{1}{2}\sqrt{(E_{m,1}-E_{m,2})^2+4\lambda^2}, \tag{26}$$

and

$$|m,-\rangle = -\cos\frac{\theta}{2}|g\rangle|1_a\tilde{m}_b\rangle + \sin\frac{\theta}{2}|e\rangle|0_a m_b\rangle, \tag{27}$$

which corresponds to the eigenenergy

$$E_{m,-} = \frac{E_{m,1}+E_{m,2}}{2} - \frac{1}{2}\sqrt{(E_{m,1}-E_{m,2})^2+4\lambda^2}, \tag{28}$$

where $E_{m,1} = \omega_a + m\omega_{M1} + \delta_1$ and $E_{m,2} = \Omega + m\omega_M$. $|e\rangle|0_a m_b\rangle$ is the eigenstate of $\tilde{H}_0$ and represents that the cavity contains no photon, the atom is in the excited state, and the membrane is in the Fock state $|m\rangle_b$. Similarly, $|g\rangle|1_a\tilde{m}_b\rangle$ represents that the cavity contains a photon, the atom is in the ground state, and the membrane is in the one-photon squeezed Fock state $|\tilde{m}\rangle_b$. The angle θ is given by $\tan\theta = \frac{2\lambda}{E_{m,1}-E_{m,2}}$. One can see that the unperturbed eigenstates $|g\rangle|1_a\tilde{m}_b\rangle$ and $|e\rangle|0_a m_b\rangle$ are modified (dressed) by the interaction between atom and cavity field.

In Fig. 3, we plot the transmission and reflection spectra for various values of g_0 in the case of $\lambda >> \Gamma$ while the membrane is initially prepared in the ground state $|0\rangle_b$. When $g_0 = 0$, the spectra show vacuum Rabi splitting [45], as shown in Fig. 3(a). Figures 3(b) and 3(c) show how the mechanical oscillator modifies the vacuum Rabi spectra with multiphonon processes taking place in the strong-coupling regime. The locations of the two zeroth-order peaks and two first-order peaks are at $\omega_k = E_{0,\pm}, E_{2,\pm}$. As g_0 becomes larger, higher-order sideband peaks will appear with interval $\sqrt{(E_{m,1}-E_{m,2})^2+4\lambda^2}$ on the right side of each main peak, corresponding to the energy levels described in Eqs. (26) and (28). Note that only even phonons can be gained or lost by the membrane due to the presence of the squeezing operator. This can be seen from the overlap between the harmonic-oscillator number state $|m\rangle_b$ and the squeezed number state $|\tilde{n}\rangle_b$ in Eq. (9). Like the case with $\lambda = 0$, we found that both the strong-coupling condition and the resolved-sideband condition ($\Gamma < \omega_M$) are required for observing sideband peaks in the Rabi splitting spectra.

As the atom-cavity coupling strength λ decreases and the condition $\lambda < \Gamma$ is satisfied, the spectra show to be analogous

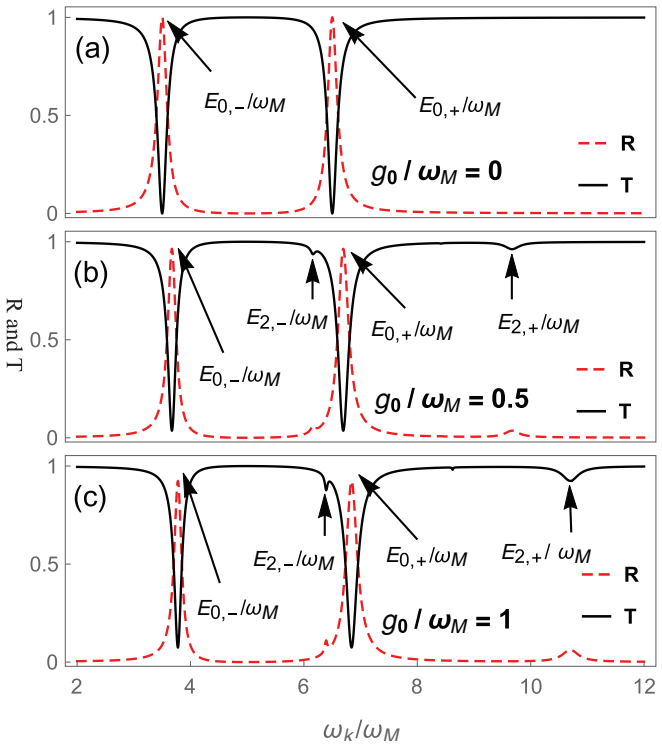

FIG. 3. Single-photon transmission spectra and reflection spectra in the case of $\lambda >> \Gamma$ for various values of g_0 with $\omega_a/\omega_M = \Omega/\omega_M = 5$, $\Gamma/\omega_M = 0.2$, $\lambda/\omega_M = 1.5$. The membrane's initial state is $|0\rangle_b$.

to that for electromagnetically induced transparency (EIT) phenomena [46]. In Fig. 4, we plot the transport spectra with $\lambda = 0.1\omega_M$ and $\Gamma = 0.2\omega_M$. Typically, when $g_0 = 0$, the spectrum exhibits a standard EIT one with a narrow transmission window. When entering the strong-coupling regime $g_0 \sim \omega_M$, sideband peaks appear in the spectra. We found that the two zeroth-order transmission dips (or reflection peaks), corresponding to the energy levels $E_{0,\pm}$, are symmetric with respect to the location of $\omega_k = (E_{0,+} + E_{0,-})/2$ with the condition $\omega_a = \Omega - \delta_1$ rather than the atom-cavity tuning condition $\omega_a = \Omega$ [47], as shown in Fig. 4(b). More generally, when $\omega_a = \Omega + 2n(\omega_M - \omega_{M1}) - \delta_1$ ($n = 0,1,2,\ldots$), we have $E_{2n,1} = E_{2n,2} = \Omega + 2n\omega_M$. Namely, the eigenstates $|e\rangle|0_a 2n_b\rangle$ and $|g\rangle|1_a\widetilde{2n}_b\rangle$ of $\tilde{H}_0$ are degenerate. This degeneracy is perturbed by the weak atom-cavity interaction $\tilde{H}_I$, resulting in a pair of near-degenerate states $|2n,-\rangle$ and $|2n,+\rangle$ with eigenenergies $E_{2n,\pm}$. In Fig. 4(c), we show that for the case of $n = 1$, the two first-order peaks exhibit EIT-like phenomena and are symmetric with respect to the location of $\omega_k = (E_{2,+} + E_{2,-})/2$. When a single-photon with frequency $\omega_k = (E_{2n,+} + E_{2n,-})/2$ is injected, destructive quantum interference occurs between the two possible transition channels $|g\rangle|0_a 0_b\rangle \to |2n,-\rangle$ and $|g\rangle|0_a 0_b\rangle \to |2n,+\rangle$, resulting in a complete transmission of the single photon. In Fig. 5, we plot the transport spectra with the atom-cavity tuning $\omega_a = \Omega$. One sees that the presence of coupling g_0 results in asymmetric peaks.

Finally, we consider the case in which the membrane is initially prepared in different states. If the initial state of the

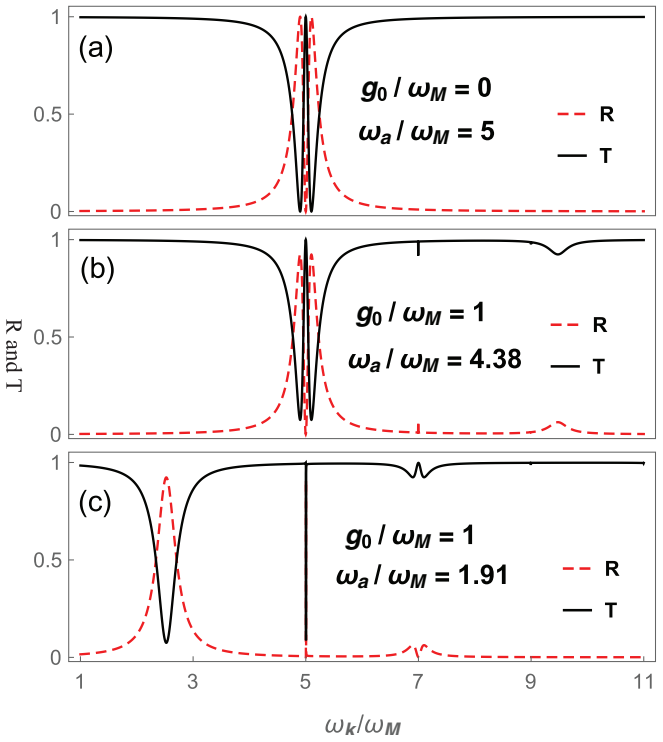

FIG. 4. Single-photon transmission spectra and reflection spectra in the case of $\lambda < \Gamma$ for various values of ω_a and g_0 with $\Omega/\omega_M = 5$, $\Gamma/\omega_M = 0.2$, $\lambda/\omega_M = 0.1$. The membrane's initial state is $|0\rangle_b$.

membrane is in odd-parity Fock states, only the odd-parity sideband peaks can be seen, while only the even-parity sideband peaks can be seen if the initial state is in even-parity Fock states. In Fig. 6, we plot the reflection spectra when the initial state of the membrane is in Fock state $|1\rangle_b$, coherent state $|\alpha\rangle_b$, and thermal state ρ_b^{th}. For the Fock state $|1\rangle_b$ in Fig. 6(a), the two main (zeroth-order) peaks are related to the transitions $|g\rangle|0_a 1_b\rangle \to |1,-\rangle$ and $|g\rangle|0_a 1_b\rangle \to |1,+\rangle$. The two first-order peaks located at $E_{3,-}/\omega_M$ and $E_{3,-}/\omega_M$ correspond

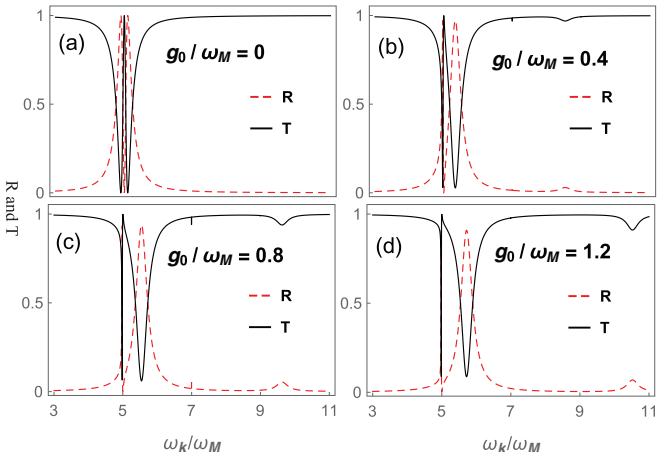

FIG. 5. Single-photon transmission spectra and reflection spectra in the case of the atom-cavity tuning $\omega_a = \Omega$ and $\lambda < \Gamma$ with various values of g_0. The parameters are $\omega_a/\omega_M = \Omega/\omega_M = 5$, $\Gamma/\omega_M = 0.2$, $\lambda/\omega_M = 0.1$. The membrane's initial state is $|0\rangle_b$.

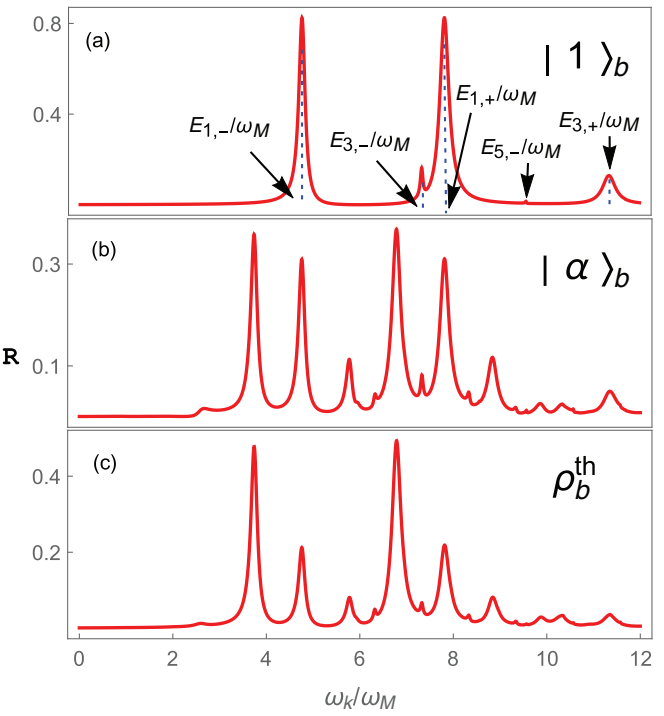

FIG. 6. Single-photon reflection spectra for various initial state of the membrane. (a) The membrane is initially prepared in the Fock state $|1\rangle_b$. (b) The membrane is initially in the coherent state $|\alpha\rangle_b$ with $\alpha = 1$. (c) The membrane is initially in the thermal state ρ_b^{th} with $\bar{n} = 1$. Other parameters are $g_0/\omega_M = 0.8$, $\Gamma/\omega_M = 0.2$, $\lambda/\omega_M = 1.5$, $\omega_a/\omega_M = 5$, $\Omega/\omega_M = 5$.

to the transitions $|g\rangle|0_a 1_b\rangle \to |3,-\rangle$ and $|g\rangle|0_a 1_b\rangle \to |3,+\rangle$. And the weak second-order peak, which is located at $E_{5,-}/\omega_M$, is related to the transition $|g\rangle|0_a 1_b\rangle \to |5,-\rangle$. The cases of coherent state $|\alpha\rangle_b$ and thermal state ρ_b^{th} are shown in Figs. 6(b) and 6(c), where it is observed that both the odd- and even-parity sideband peaks can be seen because the coherent state and thermal state contain both odd- and even-parity Fock states.

IV. DISCUSSIONS AND CONCLUSIONS

For the multimode optomechanical system, in which two optical modes are coupled to a single mechanical mode with the coupling interaction being proportional to the displacement of the mechanical oscillator, the quantum nonlinearities are enhanced when the mechanical frequencies are nearly resonant to the optical level splitting [23]. Also, the nonclassical intensity correlations in a driven, near-resonant optomechanical system consisting of two optical modes and one mechanical mode are explored [24]. In the quadratically coupled optomechanical systems, the photon blockade is examined by evaluating the second-order correlation function of the cavity photons [31].

Here, the system we consider comprises one optical mode, one mechanical mode, and a 1D waveguide. The analytical expressions for transmission and reflection spectra in this system are obtained and investigated when a single photon propagates in the one-dimensional waveguide and is scattered by the optomechanical system.

In this paper, we have studied the single-photon transport in a 1D waveguide which is coupled to a quadratic optomechanical system in the strong-coupling regime, where multiple phonons are involved in the scattering. A full quantum mechanical approach based on the Lippmann-Schwinger equation was employed to investigate the single-photon transmission and reflection properties. We analyzed the connection between the spectra and the system's energy-level structure, since the transport spectrum is not only related to the optomechanical system's energy-level structure, but also dependent on the optomechanical system's inherent parameters. One can read out the information of the mechanical system from the transport spectrum. In our treatment, we have assumed that the optical decay rate is much larger than the mechanical decay rate, so the optomechanical decoherence processes can safely be ignored.

[1] J. T. Shen and S. Fan, Opt. Lett. **30**, 2001 (2005); Phys. Rev. Lett. **95**, 213001 (2005).

[2] L. Zhou, Z. R. Gong, Y. X. Liu, C. P. Sun, and F. Nori, Phys. Rev. Lett. **101**, 100501 (2008).

[3] J. T. Shen and S. Fan, Phys. Rev. A **79**, 023837 (2009).

[4] W. Z. Jia and Z. D. Wang, Phys. Rev. A **88**, 063821 (2013).

[5] L. Neumeier, M. Leib, and M. J. Hartmann, Phys. Rev. Lett. **111**, 063601 (2013).

[6] W. Qin and F. Nori, Phys. Rev. A **93**, 032337 (2016).

[7] I.-C. Hoi, C. M. Wilson, G. Johansson, T. Palomaki, B. Peropadre, and P. Delsing, Phys. Rev. Lett. **107**, 073601 (2011).

[8] B. Dayan, A. S. Parkins, T. Aoki, E. P. Ostby, K. J. Vahala, and H. J. Kimble, Science **319**, 1062 (2008).

[9] A. Laucht, S. Putz, T. Gunthner, N. Hauke, R. Saive, S. Frederick, M. Bichler, M.-C. Amann, A. W. Holleitner, M. Kaniber, and J. J. Finley, Phys. Rev. X **2**, 011014 (2012).

[10] A. V. Akimov, A. Mukherjee, C. L. Yu, D. E. Chang, A. S. Zibrov, P. R. Hemmer, H. Park, and M. D. Lukin, Nature (London) **450**, 402 (2007).

[11] O. Astafiev, A. M. Zagoskin, A. A. Abdumalikov Jr., Y. A. Pashkin, T. Yamamoto, K. Inomata, Y. Nakamura, and J. S. Tsai, Science **327**, 840 (2010).

[12] D. E. Chang, A. S. Sorensen, E. A. Demler, and M. D. Lukin, Nat. Phys. **3**, 807 (2007).

[13] J. Claudon, J. Bleuse, N. S. Malik, M. Bazin, P. Jaffrennou, N. Gregersen, C. Sauvan, P. Lalanne, and J.-M. Gérard, Nat. Photonics **4**, 174 (2010).

[14] J. D. Teufel, T. Donner, D. Li, J. W. Harlow, M. S. Allman, K. Cicak, A. J. Sirois, J. D. Whittaker, K. W. Lehnert, and R. W. Simmonds, Nature (London) **475**, 359 (2011).

[15] A. D. O'Connell, M. Hofheinz, M. Ansmann, R. C. Bialczak, M. Lenander, E. Lucero, M. Neeley, D. Sank, H. Wang, M. Weides, J. Wenner, J. M. Martinis, and A. N. Cleland, Nature (London) **464**, 697 (2010).

[16] J. D. Teufel, D. Li, M. S. Allman, K. Cicak, A. J. Sirois, J. D. Whittaker, and R. W. Simmonds, Nature (London) **471**, 204 (2011).

[17] E. Verhagen, S. Deléglise, S. Weis, A. Schliesser, and T. J. Kippenberg, Nature (London) **482**, 63 (2012).

[18] M. Aspelmeyer, P. Meystre, and K. Schwab, Phys. Today **65**(7), 29 (2012).

[19] M. Aspelmeyer, T. J. Kippenberg, and F. Marquardt, Rev. Mod. Phys. **86**, 1391 (2014).

[20] T. Palomaki, J. Teufel, R. Simmonds, and K. Lehnert, Science **342**, 710 (2013).

[21] S. Weis, R. Rivière, S. Deléglise, E. Gavartin, O. Arcizet, A. Schliesser, and T. J. Kippenberg, Science **330**, 1520 (2010).

[22] S. Gröblacher, K. Hammerer, M. R. Vanner, and M. Aspelmeyer, Nature (London) **460**, 724 (2009).

[23] M. Ludwig, A. H. Safavi-Naeini, O. Painter, and F. Marquardt, Phys. Rev. Lett. **109**, 063601 (2012).

[24] P. Komar, S. D. Bennett, K. Stannigel, S. J. M. Habraken, P. Rabl, P. Zoller, and M. D. Lukin, Phys. Rev. A **87**, 013839 (2013).

[25] J. Thompson, B. Zwickl, A. Jayich, F. Marquardt, S. Girvin, and J. Harris, Nature (London) **452**, 72 (2008).

[26] A. M. Jayich, J. C. Sankey, B. M. Zwickl, C. Yang, J. D. Thompson, S. M. Girvin, A. A. Clerk, F. Marquardt, and J. G. E. Harris, New J. Phys. **10**, 095008 (2008).

[27] J. C. Sankey, C. Yang, B. M. Zwickl, A. M. Jayich, and J. G. E. Harris, Nat. Phys. **6**, 707 (2010).

[28] N. E. Flowers-Jacobs, S. W. Hoch, J. C. Sankey, A. Kashkanova, A. M. Jayich, C. Deutsch, J. Reichel, and J. G. E. Harris, Appl. Phys. Lett. **101**, 221109 (2012).

[29] A. Xuereb and M. Paternostro, Phys. Rev. A **87**, 023830 (2013).

[30] M. R. Vanner, Phys. Rev. X **1**, 021011 (2011).

[31] J.-Q. Liao and F. Nori, Phys. Rev. A **88**, 023853 (2013).

[32] L. F. Buchmann, L. Zhang, A. Chiruvelli, and P. Meystre, Phys. Rev. Lett. **108**, 210403 (2012).

[33] A. Nunnenkamp, K. Borkje, J. G. E. Harris, and S. M. Girvin, Phys. Rev. A **82**, 021806 (2010).

[34] W.-J. Gu, Z. Yi, L.-H. Sun, and D.-H. Xu, Phys. Rev. A **92**, 023811 (2015).

[35] E. J. Kim, J. R. Johansson, and F. Nori, Phys. Rev. A **91**, 033835 (2015).

[36] A. Rai and G. S. Agarwal, Phys. Rev. A **78**, 013831 (2008).

[37] H. Shi and M. Bhattacharya, Phys. Rev. A **87**, 043829 (2013).

[38] H. Zheng, D. J. Gauthier, and H. U. Baranger, Phys. Rev. Lett. **107**, 223601 (2011).

[39] R. J. Schoelkopf and S. M. Girvin, Nature (London) **451**, 664 (2008).

[40] J. R. Taylor, *Scattering Theory: The Quantum Theory on Nonrelativistic Collisions* (Wiley, New York, 1972).

[41] P. Zhang, L. Zhang, and W. Zhang, Phys. Rev. A **86**, 042707 (2012).

[42] M. S. Kim, F. A. M. de Oliveira, and P. L. Knight, Phys. Rev. A **40**, 2494 (1989).

[43] D. Ballester, G. Romero, J. J. Garcia-Ripoll, F. Deppe, and E. Solano, Phys. Rev. X **2**, 021007 (2012).

[44] J. Q. Liao, H. K. Cheung, and C. K. Law, Phys. Rev. A **85**, 025803 (2012).

[45] A. Wallraff, D. I. Schuster, A. Blais, L. Frunzio, R.-S. Huang, J. Majer, S. Kumar, S. M. Girvin, and R. J. Schoelkopf, Nature (London) **431**, 162 (2004).

[46] S. E. Harris, Phys. Today **50**(7), 36 (1997); M. Fleischhauer, A. Imamoglu, and J. P. Marangos, Rev. Mod. Phys. **77**, 633 (2005).

[47] P. Rice and R. Brecha, Opt. Commun. **126**, 230 (1996).